Acoustic emissions from penny-shaped cracks in glass. II. Moment tensor and source-time function

Cite as: Journal of Applied Physics **59**, 2711 (1986); https://doi.org/10.1063/1.336979
Submitted: 06 September 1985 • Accepted: 18 December 1985 • Published Online: 14 August 1998

Kwang Yul Kim and Wolfgang Sachse

Acoustic emissions from penny-shaped cracks in glass. II. Moment tensor and source-time function

Kwang Yul Kim and Wolfgang Sachse
Department of Theoretical and Applied Mechanics, Cornell University, Ithaca, New York 14853

(Received 6 September 1985; accepted for publication 18 December 1985)

In the second part of this paper we describe both epicentral and off-epicentral responses corresponding to the acoustic emission (AE) source of a Mode I type penny-shaped crack generated by the indentation technique. The characteristics of the source are described in terms of the components of the moment tensor and its time function which were recovered from the waveforms coupled with an analysis of the AE radiation pattern described in Part I of this paper [J. Appl. Phys. **59**, 2704 (1986)]. The recovered source characteristics indicate that the dominant contribution to the AE source of the penny-shaped crack comes from a single dipole acting normal to the crack plane whose temporal characteristics resemble those of a terminated parabolic ramp function.

I. INTRODUCTION

A moment tensor representation has been used for many years to model earthquake sources.[1,2] It is not surprising then to consider a similar modeling for sources of acoustic emission (AE) in materials. The moment tensor may represent any one or any linear combination of six dynamic nuclei of strains[3] which can be associated with an AE source.[4] The moment tensor is a function of space and time. A solution to the inverse source problem of AE, when the location of the source is known, refers to recovery of the magnitude of the moment tensor components and their time history.

When the size of an AE source is small in comparison with the dominant wavelength of the AE signal and the source/receiver separation, the assumption that the AE source is a point source is well justified. In most applications the moment tensor of lowest order is sufficient to represent an AE point source.[5] Furthermore, as discussed by Archambeau,[6] the radiation patterns from some nonseparable sources, for which the temporal and spatial portions of the moment tensor cannot be separated, reduce to those of the separable case for a point source.

It was shown in Part I (p. 2704) of this paper that the Mode I penny-shaped crack generated by a rigid, conical indenter is a nearly ideal point source of acoustic emission. It is assumed in this paper that such a point source of AE can be represented by a moment tensor of second rank with separable temporal and spatial dependencies. Since the tractions acting on the hypothetical crack plane point in mutually opposite directions, it is expected that a crack AE source will be modeled by a moment tensor of spatial degree one for which the monopole contribution that might arise from a change in the external loading is neglected. Furthermore, for a Mode I crack for which contributions of the shear stresses to the crack extension force are all zero,[7] the off-diagonal elements of the second-rank moment tensor representing the AE source given with respect to the principal coordinate system are likewise expected to be all zero. Hence, in this paper it will be assumed that the AE point source of a Mode I crack, and, in particular, a penny-shaped crack, can be represented by the diagonal moment tensor whose time and spatial dependencies are separable.

It will be shown in the following sections that the time function and diagonal elements of the moment tensor associated with the AE source of a penny-shaped crack can be determined from measurement of the epicentral displacement signal and the AE radiation pattern which was described in Part I of this paper.

II. ELASTODYNAMIC REPRESENTATION THEOREM FOR AN AE SOURCE

Following the work of de Hoop,[8] and Wheeler and Sternberg,[9] the displacement $\mathbf{u}(\mathbf{x},t)$ at any point $\mathbf{x}$ and time t in an elastic body V initially at rest can be expressed as the sum of the contributions from the body force $\mathbf{f}$ distributed throughout V, the surface tractions $\mathbf{T}$, and the surface displacements $\mathbf{u}_s$ on the boundary Σ of the body. Burridge and Knopoff[10] in dealing with the seismic dislocation problem showed that the surface tractions and displacements can be treated as equivalent body forces distributed over the boundary Σ. Then, the expression for $\mathbf{u}(\mathbf{x},t)$ can be written in a simplified form as

$$u_i(\mathbf{x},t) = \int_0^t d\tau \int\int\int_v f_j(\mathbf{x}',\tau)\, G_{ij}(\mathbf{x},t;\mathbf{x}',\tau) dV(\mathbf{x}')$$
$$= \int\int\int_v f_j(\mathbf{x}',\tau) * G_{ij}(\mathbf{x},t;\mathbf{x}',\tau) dV(\mathbf{x}'). \quad (1)$$

Here f_j is the component of the body force plus the body force equivalents (together called simply the body force equivalents) and G refers to the Green's function, where G_{ij} is the i,j th component of the Green's tensor. In the above equation the summation convention over the repeated indices is implied. The symbol "*" in the equation denotes a convolution integral in time. If the AE source is sufficiently small as to be treated as a point source located at ξ, the Green's function can be expanded in a Taylor series about ξ leading to

$$u_i(\mathbf{x},t) = F_j(\xi,\tau) * G_{ij}(\mathbf{x},t;\xi,\tau)$$
$$+ M_{jk}(\xi,\tau) * \frac{\partial}{\partial \xi_k} G_{ij}(\mathbf{x},t;\xi,\tau) + \cdots, \quad (2)$$

where

 0021-8979/86/082711-05$02.40

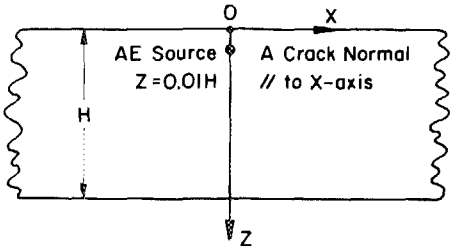

FIG. 1. Coordinate system of the AE source.

$$F_j(\xi,\tau) = \int\int\int_v f_j(\mathbf{x}',\tau)dV(\mathbf{x}'). \tag{3}$$

This term represents the j th component of the total force acting through the source volume $V(\mathbf{x}')$ and represents the monopole term. The second term is of the form

$$M_{jk}(\xi,\tau) = \int\int\int_v (x_k' - \xi_k) f_j(\mathbf{x}',\tau)dV(\mathbf{x}'), \tag{4}$$

which represents the j, k th component of the moment tensor $\mathbf{M}$ of spatial degree one.

The first term on the right-hand side of Eq. (2) can be used to describe a response resulting from a monopolar source which has zero moment. Examples include the breaking of a pencil lead[11] and the fracture of a glass capillary[12] on the surface of an elastic body. If the excitation is caused not by external forces but by the failure of the material, such as the formation of a crack, the force and its moment in the source region must be self-equilibrating. In such a case, there can be no monopole contribution to the AE source. If one disregards the contributions from higher-order multipoles, one obtains

$$u_i(\mathbf{x},t) = M_{jk} * G_{ij,k}. \tag{5}$$

For the case in which each of the components M_{jk} shares the same time function $S(t)$, one can define $M_{jk} = m_{jk} S(t)$, and Eq. (4) then becomes

$$u_i(\mathbf{x},t) = m_{jk} S(t) * G_{ij,k}. \tag{6}$$

III. AE SOURCE CHARACTERISTICS OF PENNY-SHAPED CRACKS

If the AE source of a Mode I crack, including the penny-shaped crack, is assumed to be represented by three mutually perpendicular dipoles, all sharing the same time function $S(t)$, its moment tensor $\mathbb{M}$ in the principal coordinate system can be written in matrix notation

$$\mathbb{M} = S(t)\begin{bmatrix} m_{xx} & 0 & 0 \\ 0 & m_{yy} & 0 \\ 0 & 0 & m_{zz} \end{bmatrix} = m_{xx} S(t)\begin{bmatrix} 1 & 0 & 0 \\ 0 & r_2 & 0 \\ 0 & 0 & r_3 \end{bmatrix}, \tag{7}$$

where r_2 and r_3 are defined as

$$r_2 = m_{yy}/m_{xx} \quad \text{and} \quad r_3 = m_{zz}/m_{xx}. \tag{8}$$

Substituting Eq. (7) into Eq. (6), one then obtains for the displacement

$$u_z(t) = m_{xx} S(t) * [G_{zx,x}(t) + r_2 G_{zy,y}(t) + r_3 G_{zz,z}(t)]. \tag{9}$$

The moment tensor specified by Eq. (4) depends on the orientation of the coordinate system. To avoid any ambiguity regarding the representation of the moment tensor, three coordinate axes, x, y, and z, are chosen to be parallel to the directions of the three principal stresses acting on the hypothetical crack plane prior to the formation of the penny-shaped crack, where the normal to the crack is aligned with the x axis. This is consistent with the discussion in Sec. IV of Part I of this paper. The origin of the coordinate system is taken as the point at which the indenter first makes contact with the specimen. Since the generated penny-shaped crack lies just below the surface of the specimen and typically has a size of approximately 0.01 cm in radius, the location of the corresponding AE point source is given by the coordinates x, y, z: 0, 0, 0.01 H, where H equals 1.245 cm, the thickness of the plate. This situation is illustrated in Fig. 1.

A. Time function of the AE source

In this section we describe a procedure by which the source-time function $S(t)$ of the AE source can be recovered from the detected epicentral AE signal. For a crack whose normal lies parallel to the specimen surface $S * G_{zx,x} = S * G_{zy,y}$ at epicenter, so that from Eq. (9) one obtains

$$u_z(t) = m_{xx} S(t) * [(1 + r_2)G_{zx,x}(t) + r_3 G_{zz,z}(t)]$$
$$= m_{xx}(1 + r_2)S(t) * [G_{zx,x}(t) + aG_{zz,z}(t)], \tag{10}$$

where r_2 and r_3 are as defined in Eq. (8), and

$$a \equiv \frac{m_{zz}}{m_{xx} + m_{yy}} = \frac{r_3}{1 + r_2} \quad \text{or} \quad -ar_2 + r_3 = a. \tag{11}$$

The dynamic Green's functions $G_{zx,x}$ and $G_{zz,z}$ appearing in Eq. (10), can be evaluated using the computer program developed by Ceranoglu and Pao.[13] It is assumed that the created crack surface of the AE source is transparent to the wave motion and that wave diffraction effects which may arise at the crack tip are negligibly small. This is the case in which the microcrack is small in comparison with the wavelengths of the AE signals. The effect of indenter geometry on the wave motion is also neglected because of the very small contact area between the indenter and the specimen.

Measurement of the normal displacement signal $u_z(t)$ at epicenter, is made with a normal displacement-sensitive AE transducer. The results to be described were obtained with a self-aligning capacitive transducer, details of which are described elsewhere.[14] To assess the fidelity of this transducer as a normal displacement sensor, its epicentral response to a step excitation obtained by the fracture of a glass capillary on the opposite side of the specimen is compared to the waveform computed for a step normal force excitation. The close agreement between measured and synthesized waveforms shown in Fig. 2 indicates that this transducer is operating as an excellent displacement transducer. The rise time associated with the first P-wave arrival of the signal was measured to be less than 0.1 μs. For comparison, we show in Fig. 3(a) the displacement signal detected by the same transducer at the epicentral receiver point resulting from the formation of a penny-shaped crack. The data is that obtained from crack no. 9 listed in Table I.

From the measured displacement signal $u_z(t)$ and the

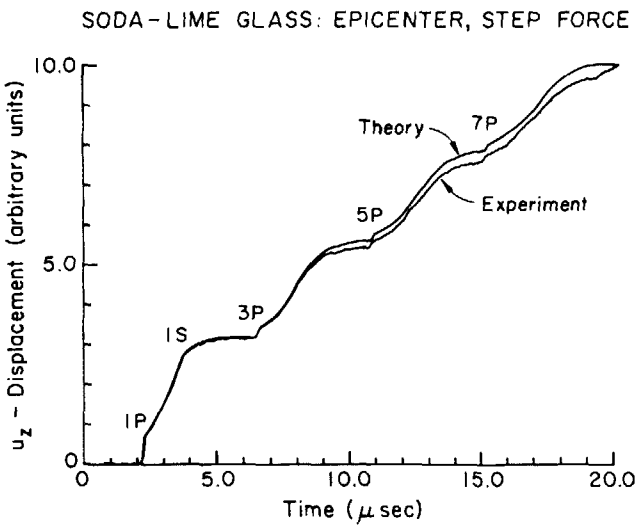

FIG. 2. Observed and computed displacement signals at epicenter from a step normal force excitation.

Green's functions $G_{zx,x}(t)$ and $G_{zz,z}(t)$, the values of the moment tensor ratio a, and the source-time function $S(t)$, appearing in Eq. (10) were computed with the double-iterative least-squares algorithm.[15] The recovered source-time function $S(t)$ for crack no. 9 is shown in Fig. 4. It resembles a terminated parbolic ramp function except for the initial dip occurring before 0.1 μs. The rise time of the source-time function is determined to be about 0.2 μs. The values of the ratio a in Eq. (10) are listed in Table I for three AE events corresponding to the formation of penny-shaped cracks.

Using the value of the ratio a and the source-time function, $S(t)$, the normal displacement at epicenter was synthesized for crack no. 9. Comparison is made in Fig. 3(b)

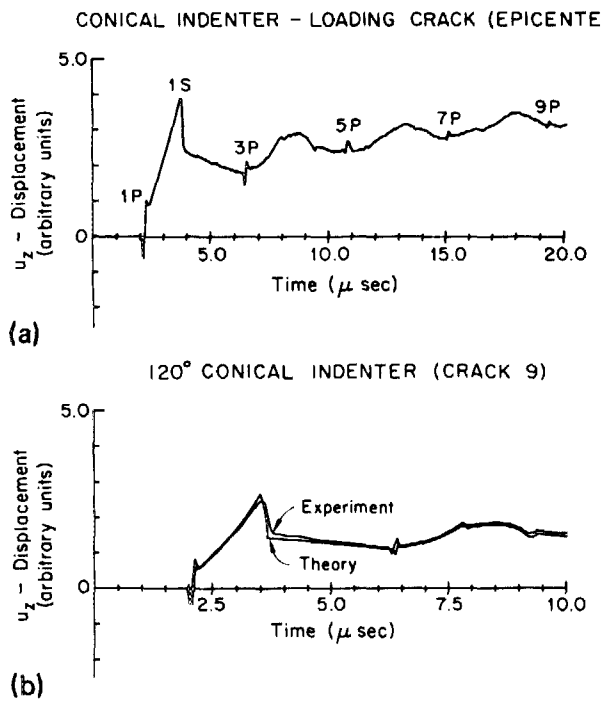

FIG. 3. (a) Detected displacement signals at epicenter from a penny-shaped crack (crack no. 9). (b) Comparison between synthesized and observed crack signals.

TABLE I. The values of the ratio a [see Eq. (10)].

Crack no.	8	9	10
a	0.081	0.052	0.049

between the synthesized and the measured waveforms. They are seen to be in excellent agreement with each other. The value of a is generally much less than 1.0, indicating that a single, horizontal dipole replicates the experimental curve except for the small wriggles at the P-wave arrivals.

The signal displayed in Fig. 3(a) was reproducibly obtained for many penny-shaped cracks. The average value of the ratio a listed in Table I is 0.061 ± 0.020. This value is used in the next section to determine the values r_2 and r_3 appearing in Eq. (9) for the cracks listed in Table II of the first part of this paper. This is justified because the value of a falls within the prescribed error limit for the various cracks.

B. Moment tensor of the AE source

In Part I of this paper the radiation pattern was obtained from the amplitude data of the signals detected by piezoelectric transducers located at various angular positions at a distance of 2.066 H (H is the thickness of the plate) from the epicenter. Here it is shown how the components of the moment tensor can be recovered from the radiation pattern associated with only the amplitude of the first arrival signal, that is the 1P-wave amplitude, when combined with the epicentral response as discussed in the previous section. The basis of the method can be illustrated with synthetic waveforms.

Synthetic, off-epicentral displacement signals at the zero degree angular location were computed by convolving the dynamic Green's functions $G_{zx,x}$, $G_{zy,y}$, and $G_{zz,z}$ in Eq. (9) corresponding to a source consisting of three mutually perpendicular dipoles with the source-time function $S(t)$. The latter was that recovered from the epicentral waveform of a crack. An example based on the results from crack no. 9 is shown in Fig. 5. As can be seen in this figure, $S(t)^* G_{zy,y} = 0$ at the time of the 1P-arrival. An analytical expression

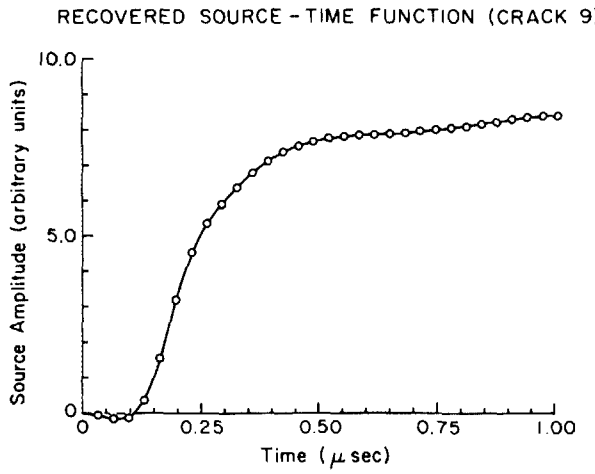

FIG. 4. Recovered source-time function for crack no. 9.

TABLE II. Normalized component of the moment tensor of various cracks.

Crack no.	m_{yy}/m_{xx}	m_{zz}/m_{xx}
1	0.072 ± 0.006	0.065 ± 0.022
2	0.126 ± 0.005	0.069 ± 0.023
3	0.147 ± 0.006	0.070 ± 0.023
4	0.155 ± 0.006	0.070 ± 0.023
5	0.179 ± 0.005	0.072 ± 0.024
6	0.035 ± 0.006	0.063 ± 0.021
7	0.070 ± 0.006	0.065 ± 0.022

for the displacement amplitude at the 1P-wave arrival for this source/receiver configuration can be obtained by substituting this result into Eq. (9) and combining it with Eq. (8) of Part I of this paper. The result is

$$u_z(\theta = 0°) = m_{xx}\{[S(t)^* G_{zx,x}(t)]_{\theta=0} + r_3[S(t)^* G_{zz,z}(t)]\} = c(b+1). \quad (12)$$

The corresponding displacement amplitude at the receiver located at 90° to the normal of the crack plane is obtained by rotating the coordinate axes by 90° about the z axis, resulting in

$$u_z(\theta = 90°) = m_{xx}\{r_2[S(t)^* G_{zx,x}(t)]_{\theta=0} + r_3[S(t)^* G_{zz,z}(t)]\} = cb. \quad (13)$$

The ratio

$$[S(t)^* G_{zz,z}(t)]/[S(t)^* G_{zx,x}(t)]_{\theta=0}$$

evaluated at the 1P-wave arrival was found to be equal to -0.277 for the signals depicted in Fig. 5. Similar values were found for the other crack signals analyzed. If Eq. (12) is divided by Eq. (13), one finds after a little manipulation,

$$(1+b)r_2 - 0.277\, r_3 = b. \quad (14)$$

Expressions for the moment tensor ratios r_2 and r_3 are obtained in terms of the ratio a and the constant b if Eq. (11) is combined with Eq. (14). Thus,

$$r_2 = \frac{0.277\, a + b}{1 - 0.277\, a + b}, \quad r_3 = \frac{a(1+2b)}{1 - 0.277\, a + b}. \quad (15)$$

Using the average value of the ratio a given earlier, the ratios r_2 and r_3 were computed for each of the penny-shaped cracks listed in Table II of the preceding paper. The normalized components of the moment tensor with respect to m_{xx} recovered for these cracks from their emitted signals are listed in Table II.

Inspection of the results given in Table II shows that the dominant contribution to the AE source of the penny-shaped crack arises from m_{xx} which corresponds to a single dipole aligned normal to the crack plane. This is as expected from a fracture mechanics analysis for Mode I cracks. In assigning error limits for r_2 and r_3, the errors associated with the constant b appearing in Eq. (15) were not taken into account. The stated error bounds are due solely to the errors associated with the quantity a. Since b was obtained from evaluation of the radiation pattern of the AE signals, determination of this quantity from signals which are not displacement signals may lead to significant errors. A typical relative error $\Delta b/b$ was estimated from the nonlinear least-squares curve fitting algorithm to be around 0.2. This does not include any systematic or random errors which are difficult to estimate. The typical values of a and b are about 0.06 and 0.1, respectively. Thus, the errors in r_3 can be approximated by the error in the value of a, while the error in r_2 by the error in b. Therefore, the values of r_3 ($= m_{zz}/m_{xx}$) listed in Table II are believed to be more reliable than those for r_2 ($= m_{yy}/m_{xx}$). If a more substantial reduction in the error of the value b is sought, displacement sensors should also be used for the radiation pattern measurements.

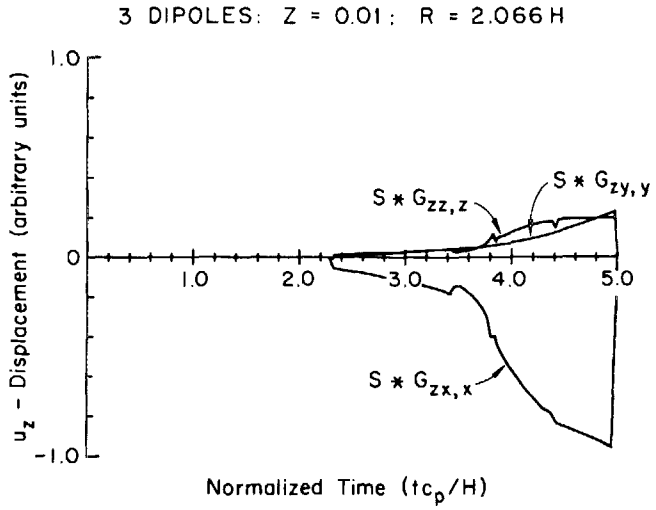

FIG. 5. Computed off-epicentral responses corresponding to three mutually perpendicular dipole sources.

IV. DISCUSSION

Initially, the AE source was assumed to be represented by a linear combination of three mutually perpendicular dipoles, but our experimental results have shown that the dominant contribution in the AE source of a Mode I crack in glass specimens is due principally to a single dipole acting normal to the crack plane. This result is not unexpected from a fracture mechanics analysis of the formation of a Mode I crack in a brittle solid which is adequately discussed in a number of textbooks.[7,16] The formation of a crack in such materials is modeled as a sequence of an imaginary cutting through the crack plane and a removal of the imposed tractions acting on the cut plane. For a Mode I crack for which the tractions are normal to the crack plane, the removal of the imposed tractions comprises a tensile dipole. The experiments described here have demonstrated that this model is applicable to represent the AE source from a penny-shaped crack in glass specimens.

For ductile materials such as steel and aluminum, the formation of a crack is preceded by the formation of the nonlinear plastic zone. Energy release during the formation of a crack is not exclusively confined to the crack surface but occurs through the nonlinear zone. In this case it can be expected that the AE source is a volume source. Evaluation of such AE sources requires a detailed knowledge of the nonlinear zone. If, however, one were to assume that the nonlinear zone is confined to lie within a narrow, slitlike region immediately ahead of the crack tip, one can adapt Dug-

dale's[17] model. In that case, the AE source volume can then be identified as the product of the crack area and the narrow width of the plastic zone. The linkage distance of a dipole, normal to the crack plane, may be interpreted as the width of the nonlinear zone in the ductile material, but it reduces to one interatomic spacing in a perfectly brittle solid.

V. CONCLUSIONS

Based on the experiments and analysis described in this paper, the following conclusions can be drawn. First, an AE source-time function of the penny-shaped crack resembles a terminated parabolic ramp. Second, the dominant contribution to the AE source of the penny-shaped crack (or a Mode I crack in brittle solids) comes from a dipole acting normal to the crack plane as expected from a point of view of fracture mechanics for a Mode I crack. This work demonstrates the feasibility of quantitative acoustic emission measurements to investigate dynamic fracture processes in materials.

ACKNOWLEDGMENT

This work was supported by the National Science Foundation through grants to the Materials Science Center and the College of Engineering at Cornell University. This support is greatly acknowledged.

[1]F. Gilbert, Geophys. J. R. Astron. Soc. **22**, 223 (1970).
[2]D. J. Doornbos, in *Identification of Seismic Sources—Earthquake or Underground Explosion*, edited by E. S. Husebye and S. Mykkeltveit (Reidel, New York, 1981), pp. 207–232.
[3]A. E. H. Love, *A Treatise on the Mathematical Theory of Elasticity* (Cambridge University, Cambridge, 1927), pp. 186–189.
[4]Y. H. Pao, "Theory of Acoustic Emission," in *Elastic Waves and Nondestructive Testing of Materials*, edited by Y. H. Pao (ASME, New York, 1978), AMD-Vol. 29, pp. 107–128.
[5]G. Bachus and M. Mulcahy, Geophys. J. R. Astron. Soc. **46**, 341 (1976).
[6]C. B. Archambeau, Rev. Geophys. **6**, 241 (1968).
[7]B. R. Lawn and T. R. Wilshaw, *Fracture of Brittle Solids* (Cambridge University, Cambridge, 1975), Chap. 3.
[8]A. T. de Hoop, Doctoral Dissertation, Technische Hogeschool, Delft (1958).
[9]L. T. Wheeler and E. Sternberg, Arch. Rational Mech. Anal. **31**, 51 (1968).
[10]R. Burridge and L. Knopoff, Bull. Seis. Soc. Am. **54**, 1875 (1964).
[11]N. N. Hsu and S. Hardy, in *Elastic Waves and Nondestructive Testing of Materials*, edited by Y. H. Pao (ASME, New York, 1978), AMD-Vol. 29, pp. 85–106.
[12]R. F. Breckenridge, C. E. Tschiegg, and M. Greenspan, J. Acoust. Soc. Am. **57**, 626 (1975).
[13]A. N. Ceranoglu and Y. H. Pao, J. Appl. Mech. **48**, 125, 133, 139 (1981).
[14]K. Y. Kim and W. Sachse, Rev. Sci. Instrum. **57**, 264 (1986).
[15]J. E. Michaels and Y. H. Pao, J. Acoust. Soc. Am. **77**, 2005 (1985).
[16]H. L. Ewalds and R. J. H. Wanhill, *Fracture Mechanics* (Edward Arnold, London, 1984), Chap. 2.
[17]D. S. Dugdale, J. Mech. Phys. Solids **8**, 100 (1960).